# Arc Modelling for Switching Performance Evaluation in Low-Voltage Switching Devices

Dongkyu Shin*, Igor O. Golosnoy
School of Electronics and Computer Science
University of Southampton
Southampton, SO17 1BJ, UK
* ds7g14@soton.ac.uk

John W. McBride[1,2]
[1]Faculty of Engineering and the Environment
University of Southampton, Southampton, SO17 1BJ, UK
[2]University of Southampton Malaysia Campus
Nusajaya, 79200, Johor, Malaysia

***Abstract*— Arc modelling is an efficient tool for predicting the switching performance of low-voltage switching devices (LVSDs) prior to testing real products. Moreover, it offers a valuable design aid in the improvement and optimization of LVSDs. This paper focuses on the investigation of evaluators that predict re-ignition phenomena and the numerical simulation of arc characteristics in LVSDs. It is found that the probability of re-ignition depends strongly on the ratio of the system voltage to the exit-voltage. The implemented 3-D arc model is based on conventional magnetohydrodynamics theory and takes into account the properties of air that vary with temperature and pressure, motion of the contact, arc root formation and plasma radiation. The simulated results are compared with experimental data to validate the proposed arc model and the voltage trends show agreement.**

***Keywords—arc modelling, re-ignition, low-voltage switching devices, magnetohydrodynamics (MHD)***

## I. INTRODUCTION

Low-voltage switching devices (LVSDs) are essential to turn on and off electric current and to protect humans and other connected equipment against overload or short circuit accidents in the power distribution network. A quenching chamber of a LVSD is the main volume for switching current and consists of a movable and fixed contact, magnetic yoke, arc runner, splitter plates and vents, as shown in Fig. 1. When the movable contact separates from the fixed contact, an arc is established between the contacts that elongates as the contact gap increases. Gas flow and the magnetic Lorentz force then drive the arc toward the splitter plates. Concurrently, there is a dramatic increase in the arc voltage between contacts due to the multiple anodic and cathodic voltage drops in the splitter plates. Ideally, the arc is extinguished at the first current zero moment, however the arc can re-ignite beyond this point. During this breaking process, the arc parameters have a great influence on interruption performance of the LVSD [1]. If parameters such as the voltage, current and motion of the arc can be accurately calculated and evaluators of re-ignition determined, we can predict and improve the switching performance of LVSDs through an arc simulation.

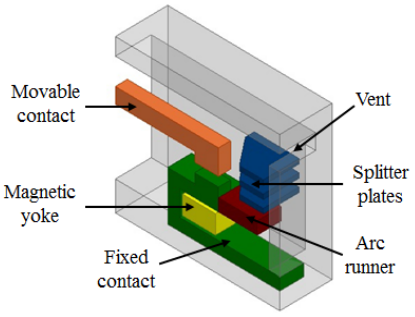


Fig. 1. Half symmetric schematic structure of a quenching chamber.

There has been several reports on correlations between the experimentally observed behaviour of the arc and predicted performance of LVSDs. McBride et al. carried out experimental studies of the influence of contact opening velocity and material, wall material and venting condition on the arc motion in a miniature circuit breaker (MCB) using a fibre optic imaging system, pressure gauges and spectrography [2]. Balestrero et al. introduced several 'microscopic evaluators' that can predict re-ignition by measuring the arc current or arc voltage over a 10 μs time period near the current zero event, when ion recombination and non-equilibrium phenomena dominate [3]. Hauer et al. found that the probability of re-ignition after the current zero event is heavily dependent on the 'exit-voltage' (the arc voltage immediately prior to the current zero event) [4], which can be calculated through an arc simulation. Hauer's methodology can be used in a 2-step design procedure: firstly, to establish the arc threshold voltage and secondly, to simulate the arc characteristics up to the current zero moment. The advantage of such an approach is that the complex simulation of plasma processes during arc re-ignition is not required.

Arcs are non-linear phenomena and their characteristics are strongly dependent on the length, temperature, pressure and attachment points of the arc. For the reliable prediction of the switching performance of LVSD, the arc behaviour should be accurately modelled. In terms of the arc simulation, Karetta et al. analyzed the arc motion with a 3-D magnetohydrodynamics (MHD) model incorporating heat conduction, gas and current flows and magnetic force [5]. Lindmyer et al. proposed arc modelling method that includes the arc root formation on the splitter plates by using a thin layer of current-dependent resistive material [6]. Rong and Ma et al. conducted numerical

analysis on the influence of metal erosion and wall ablation on arc behaviour in a LVSD [7], [8].

Although technology available for the design and analysis of LVSDs has been notably developed thanks to the previous experimental and numerical studies, there are still limitations in the prediction of the switching performance and optimization of LVSDs. The experimental approach is very expensive and time-consuming. Moreover, it is difficult to obtain experimentally internal arc parameters such as gas velocity, current density and temperature that are useful in improving the design of LVSDs. Most previous numerical methods have focused on the behaviour of the arc plasma prior to the current zero moment without evaluating the probability of re-ignition following the current zero moment, even though avoiding re-ignition is a key goal when designing the quenching chamber of a LVSD.

This paper presents a reliable evaluator which can predict re-ignition following the current zero point and the numerical simulation of arc behaviour prior to the current zero event based on 3-D MHD arc modelling. The model presented in this paper takes into account the properties of air that vary with temperature and pressure, contact motion, arc root formation and plasma radiation. The simulation results are compared with the experimental data to validate the proposed arc model.

## II. Experiments on Arc Re-ignition

### A. Experimental Setup

The experimental investigation for predicting re-ignition is carried out by two types of interruption tests. One is a low power test of a single pole MCB with 10 kA current and 252 V phase voltage. The other is a higher power test for a three pole moulded case circuit breaker (MCCB) with 20 kA current and 483 V line-to-line voltage. Fig. 2 shows an equivalent test circuit for a single pole MCB and three pole MCCB. Energy is supplied via a 13.8 kV commercial power line whose voltage and current are adjusted by a transformer, resistors and reactors to the test circuit. For single pole tests, only two phases of the test circuit are used as shown in Fig. 2 (a). The current and voltage waveforms are collected on every interruption test by an oscilloscope.

### B. Experimental Results

Fig. 3 shows the voltage and current waveforms for both a successful and failed interruption of the two types of MCBs under the same test condition, when the system voltage is 252 V, the prospective current is 10 kA and the power factor is 0.45. The successful interruption means that short circuit current is interrupted at the first current zero point whereas failed one indicates there is re-ignition after the first current zero. During a successful interruption, the arc voltage reaches a relatively high value (> 400 V) compared to the voltage in a failed interruption, and remains high until the current zero point. In contrast, a failed interruption has a lower and significantly less stable arc voltage and notably lower exit-voltage. If the LVSD fails to interrupt the short circuit current at the first current zero (shown in Fig. 3 (b)), the arc current continues to flow until next current zero and the large current and a long arcing duration cause severe damage to the device. It is clear from Fig. 3 that the switching performance of LVSDs is affected by arc characteristics and there is a distinct difference in the arc voltage waveforms between successful and failed tests.

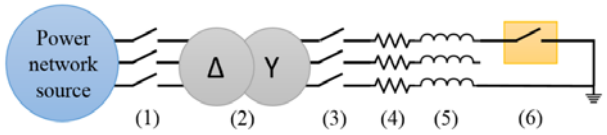


(a) Single phase test for a MCB

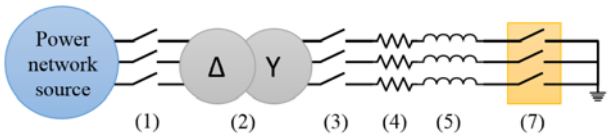


(b) Three phases test for a MCCB

Fig. 2. Equivalent test circuits for the MCB and MCCB: (1) back-up circuit breaker, (2) three phase transformer, (3) making switch, (4) resistor, (5) reactor, (6) test MCB, (7) test MCCB.

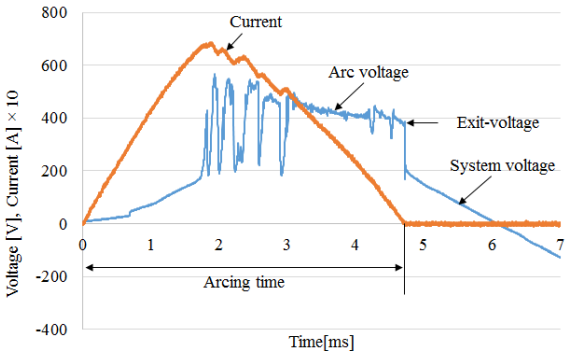


(a) Successful interruption test

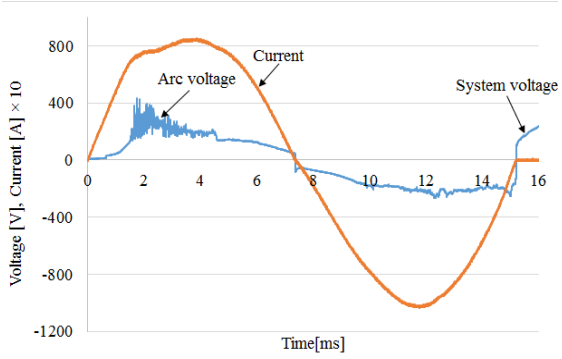


(b) Failed interruption test

Fig. 3. Voltage and current waveforms during interruption operation of MCBs.

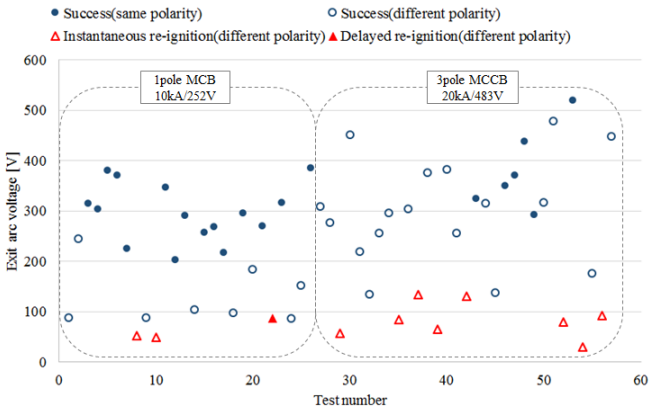


Fig. 4. Relation between interruption performance and exit-voltage.

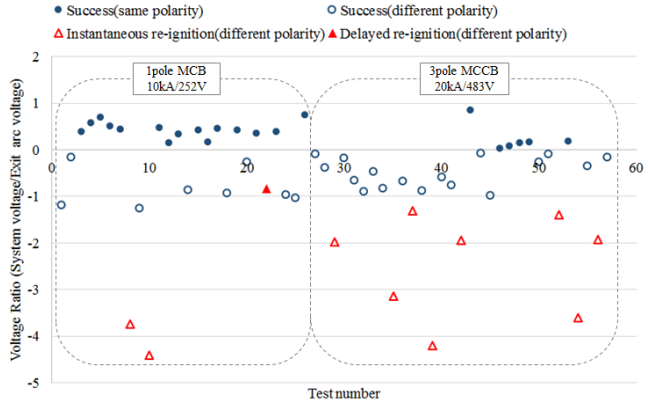


Fig. 5. Relation between interruption performance and voltage ratio.

Figs. 4 and 5, respectively, illustrate the interruption performances of MCBs and MCCBs that are analysed by the exit-voltage and the voltage ratio, which is calculated by the exit-voltage and system voltage at the first current zero instant as given (1)

$$Voltage\ ratio = V_{system}(t_0) / V_{exit}\ , \qquad (1)$$

where $t_0$ is the instant of the first current zero, $V_{exit}$ is the exit-voltage and $V_{system}$ is the system voltage, obtained through extrapolation from the first zero point of the system voltage after $t_0$. Re-ignition in interruption tests can be further classified as one of two types [4]: 'instantaneous' re-ignition, which occurs immediately after the current zero event causing the short circuit current continue to flow in reverse polarity and 'delayed' re-ignition, where there is a pause between the current zero moment and re-ignition. In addition, there are two possible cases: arc voltage and system voltage may have the same (shown in Fig 3 (a)), or opposing polarities.

In Fig. 4, it can be seen there is a different threshold of the exit-voltage that distinguishes successful interruption from failed interruption in MCB and MCCB tests. For the MCB test if the exit-voltage is above 86 V, the arc can be interrupted at the first current zero. However, for the MCCB test, the threshold is 134V. These results illustrate that re-ignition phenomenon is strongly correlated to the exit-voltage and its value varies with the interruption test condition.

The voltage ratio is an alternate evaluator as shown in Fig. 5. If the exit-voltage is higher than the system voltage and their polarities are the same, the interruption test is always successful. This situation happens only when the arc moves quickly towards splitter plates and the arc voltage is high enough to make the current zero moment occur prior to the zero point of the system voltage. In addition, there is a global threshold evaluator that predicts re-ignition under the two interruption regimes (single pole MCBs under 10 kA, 252 V and three pole MCCBs under 20 kA, 483 V) tested in this study. If the voltage ratio is higher than -1.3 and less than 0, the probability of the successful interruption is around 96%. However, of the 26 interruption trials a single delayed re-ignition was observed that was not predicted by this evaluator.

## III. Numerical Model and Simulation Results

### A. Assumptions and Simplifications for Arc Model

To reduce the complexity of the arc model in a LVSD, the following assumptions and simplifications have been adopted.

- The arc column is considered to be in a state of local thermodynamic equilibrium (LTE).
- The arc is modelled initially as a hot channel in a small gap between contacts which has a homogenous temperature distribution.
- The arc gas motion is regarded as a laminar flow.
- Metal erosion and wall ablation are not taken into account in the arc model.
- The splitter plates are considered to behave as linear ferromagnetic materials.

### B. MHD Equations in Arc Column

The arc column is electrically neutral and a mixture of electrons and heavy particles (ions, atoms and molecules) in thermal equilibrium at high temperature. If the assumption of LTE holds in the arc column, the arc can be treated as a single fluid and the mass, momentum and energy conservation equations can describe the relation between the velocity, pressure, temperature in the arc column as given below [5], [10],

$$\frac{\partial \rho}{\partial t} + \nabla \cdot \left( \rho \vec{V} \right) = 0\ , \qquad (2)$$

$$\frac{\partial \left( \rho v_i \right)}{\partial t} + \nabla \cdot \left( \rho v_i \vec{V} \right) = -\nabla p + \nabla \cdot \left( \eta \nabla v_i \right) + \left( \vec{J} \times \vec{B} \right)_i\ , \qquad (3)$$

$$\frac{\partial \left( \rho H \right)}{\partial t} + \nabla \cdot \left( \rho H \vec{V} \right) = \nabla \cdot \left( \frac{\lambda}{c_p} \nabla H \right) + \frac{\partial p}{\partial t} + \sigma E^2 + S_{rad} + S_{\eta}\ . \qquad (4)$$

In the previous equations, $\rho$ is the density ($kg/m^3$), $t$ is the time ($s$), $\vec{V}$ is the velocity (m/s), $v_i$ is the velocity component in $i$

direction, $p$ is the pressure ($Pa$), $\eta$ is the dynamic viscosity ($kg/(m{\cdot}s)$), $\vec{J}$ is the current density ($A/m^2$), $\vec{B}$ is the magnetic flux density ($T$), $H$ is the dynamic plasma enthalpy ($J/kg$) expressed by $h+\vec{V}^2/2$, $h$ is the static enthalpy ($J/kg$) determined by $\int c_p dT$, $\lambda$ is the thermal conductivity ($W/(m{\cdot}K)$), $c_p$ is the specific heat capacity ($J/(kg{\cdot}K)$), $\sigma$ is the electrical conductivity ($S/m$), $E$ is the electric field intensity ($V/m$), $S_{rad}$ is the radiation energy source ($W/m^3$) and $S_\eta$ is the heat due to viscous dissipation ($W/m^3$).

The electric field $\vec{E}$, which determines the ohmic heating source in the energy equation, is calculated from Gauss's law, (5) and (6),

$$\nabla \cdot \left( \sigma \nabla \Phi \right) = 0 , \tag{5}$$

$$\vec{E} = -\nabla \Phi , \tag{6}$$

where $\Phi$ is the electric scalar potential ($V$).

Moreover, $\vec{J}$ and $\vec{B}$, which are used to calculate the Lorentz force in the momentum equation, are obtained from the following equations,

$$\vec{J} = \sigma \vec{E} , \tag{7}$$

$$\nabla^2 \vec{A} = -\mu \vec{J} , \tag{8}$$

$$\vec{B} = \nabla \times \vec{A} , \tag{9}$$

where $\vec{A}$ is the magnetic vector potential ($Wb/m$) and $\mu$ is the permeability ($H/m$).

The simplified net emission coefficient method is employed in this work to calculate the radiation energy losses due to its simplicity, and the net emission coefficients are computed from (10),

$$\varepsilon = C_1 \left( \exp\left(C_2 T\right) - \exp\left(C_2 T_r\right) \right) , \tag{10}$$

where $C_1$ and $C_2$ are the constant coefficients 300 $W/m^3$ and 0.0011 $K^{-1}$ respectively, $T_r$ is the ambient temperature and $T$ is the arc temperature [10].

### C. Numerical Model for Arc Root

The arc root is a thin region between the arc column and the metal surface of the cathode or anode. Before entering the splitter plates, the arc gradually bends and stretches around the plates generating excessive voltage that is necessary to form arc roots on the splitter plates [6]. The voltage drops in the arc roots on the cathode and anode are relatively high compared to that in the arc column. This arc root formation plays an important role in the arc behaviour before the current zero and the value of the exit voltage used to calculate the evaluator for re-ignition after the current zero point. In order to consider the arc root area, special arc root modelling method is needed because LTE condition does not hold in the arc root and ordinary MHD theory cannot simulate the arc root phenomena [10].

The relationship between voltage and current density as shown Fig. 6 (a) is modelled as nonlinear in the arc root region in order to take into account the arc splitting phenomenon on the splitter plates and the high arc voltage in the arc root [6]. Moreover, the resistivity in the arc root is modelled to vary with distance from the cathode or anode surface as shown in Fig. 6 (b).

### D. Simulation Results

The arc modelling process (Fig 7) comprises of procedures of arc ignition, MHD simulation of the plasma, contact motion and evaluating the probability of re-ignition. The MHD calculation includes subroutines for the computation of radiation losses and formation of the arc root. The arc modelling is performed in the Ansys CFX commercial software package used in previous studies [6], [10].

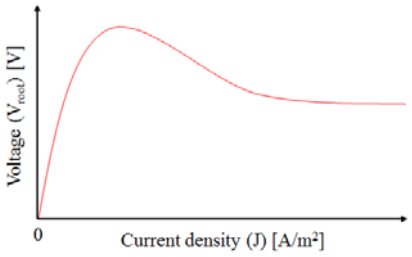


(a) Relation between voltage and current density

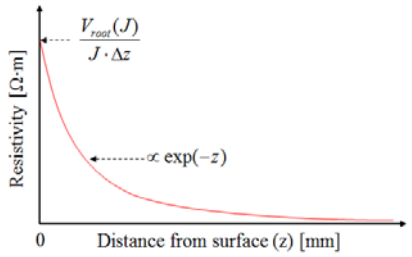


(b) Relation between resistivity and distance

Fig. 6. Modelling method for the arc root.

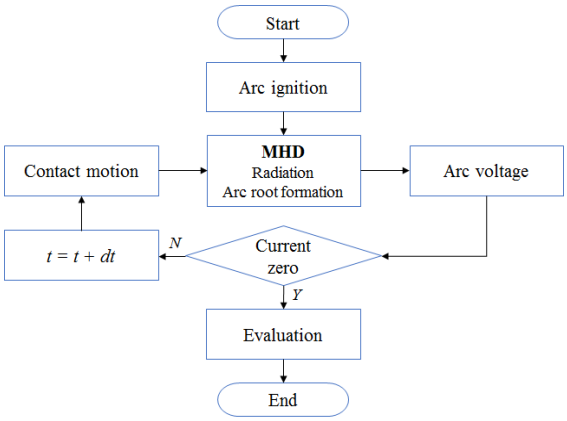


Fig. 7. Diagram of the arc modelling process.

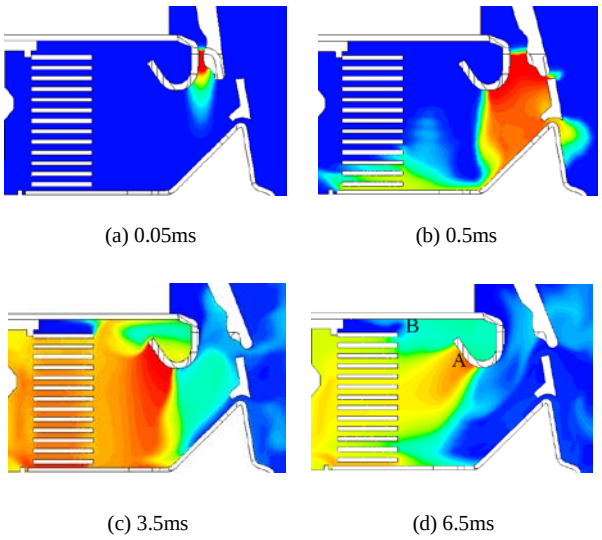


(a) 0.05ms (b) 0.5ms

(c) 3.5ms (d) 6.5ms

Fig. 8. Temperature distribution in the quenching chamber of the MCB.

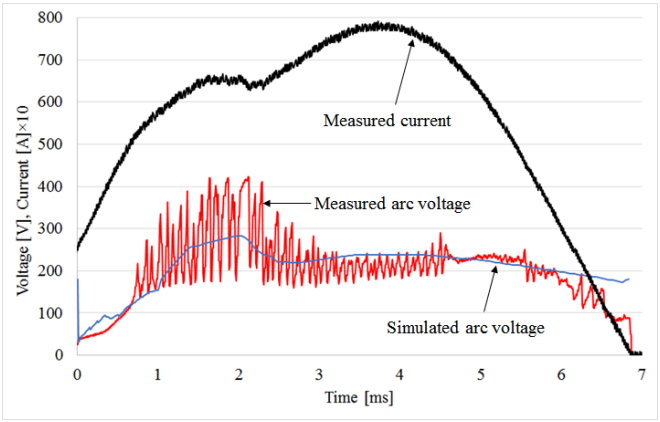


Fig. 9. Comparison between experimental and simulation results of the MCB.

Fig. 8 illustrates the predicted arc temperature distribution on the symmetry plane in the quenching chamber of the MCB when the measured current flows through the MCB (see Fig. 9 for comparison with experiments). At the beginning of the simulation, the arc is modelled as a hot cylinder channel between contacts, with 1mm radius and 10,000 K temperature, and then it moves from the ignition contact area toward the splitter plates by the gas convective flow and the Lorentz force. Afterward, the arc is divided into multiple segments by the plates and a high arc voltage is generated between the contacts. The simulated results illustrate that the arc roots on the fixed contact stays at the 'A' site without moving to 'B' site (Fig. 8 (d)). This leads to a low arc voltage and long arcing duration, as shown in Fig. 9. If the arc root rapidly relocates from the 'A' to the 'B' site, the increase in arc voltage is greater and the simulated switching performance is enhanced. This indicates a potential ways for the design modifications.

### *E. Validation of Arc Simulation*

Fig. 9 shows the comparison between experimental and predicted electric characteristics of the arc while the measured current flows through the MCB. In general, the computed and experimental voltages show the same trend although there are some differences at the initial stage and at the end of the interruption process. These discrepancies could be caused by the simplification of the ignition process or the absence of wall ablation and metal erosion in the arc model.

## IV. CONCLUSIONS

The experimental investigations of evaluators for re-ignition and the numerical modelling on arc behaviour in LVSDs have been studied in this paper. The following conclusions can be drawn:

- The interruption test results support the concept that re-ignition phenomenon after the current zero moment is strongly correlated to the ratio of the exit-voltage to system voltage.
- The arc simulation based on the 3-D MHD approach and the arc root model has been implemented and validated.
- Accurate arc modelling on splitter plates and especially around the current zero moment are necessary to reliably predict the switching performance. It is a part of ongoing research.

## REFERENCES

[1] P. Freton and J.J. Gonzalez, "Overview of current research into low-voltage circuit breakers, " The Open Plasma Physics Journal, Vol. 2, pp 105–119, 2009.

[2] J. W. McBride, K. Pechrach, and P. M. Weaver, "Arc motion and gas flow in current limiting circuit breakers operating with a low contact switching velocity, " IEEE Transactions on Components and Packaging Technologies, Vol. 25, no. 3, pp 427–433, 2002.

[3] A. Balestrero, L. Ghezzi, M. Popov, and L. Van Der Sluis, "Current interruption in low-voltage circuit breakers, " IEEE Transactions on Power Delivery Vol. 25, no. 1, pp 206–211, 2010.

[4] W. Hauer and X. Zhou, "Re-ignition and post arc current phenomena in low voltage circuit breaker," Proceedings of the 27th International Conference on Electrical Contacts, pp 398–403, 2014.

[5] F. Karetta and M. Lindmayer, "Simulation of the gasdynamics and electromagnetic processes in low voltage switching arc," IEEE Transactions on Components, Packaging, and Manufacturing Technology, Vol. 21, no. 1, pp 96–103, 1998.

[6] M. Lindmayer, E. Marzahn, A. Mutzke, T. Rüther, and M. Springstubbe, "The process of arc splitting between metal plates in low voltage arc chutes," IEEE Transactions on Components and Packaging Technologies, Vol. 29, no. C, pp 310–317, 2006.

[7] M. Rong, Q. Ma, Y. Wu, T. Xu, and A. B. Murphy, "The influence of electrode erosion on the air arc in a low-voltage circuit breaker," Journal of Applied Physics, Vol. 106, no. 2009, 2009.

[8] Q. Ma, M. Rong, A. B. Murphy, Y. Wu, and T. Xu, "Simulation study of the influence of wall ablation on arc behaviour in a low-voltage circuit breaker," IEEE Transactions on Plasma Science, Vol. 37, no. 1, pp 261–269, 2009.

[9] F. Yang, Y. Wu, M. Rong, H. Sun, A. B. Murphy, Z. Ren, and C. Niu, "Low-voltage circuit breaker arcs - simulation and measurements," Journal of Physics D: Applied Physics, Vol. 46, no. 27, 2013.

[10] A. I. Aio, "Modelization and analysis of the electric Arc in low voltage circuit breakers," PhD thesis, Universidad del País Vasco Euskal Herriko Unibertsitatea, 2013.